

Metallurgical characterization of kaolin from Atacama, Chile

<http://dx.doi.org/10.1590/0370-44672016690005>

Oscar Rivera

Ingeniero Metalurgista
Universidad de Atacama
Departamento de Ingeniería en Metalurgia
Copiapó - Atacama - Chile
oscar.rivera@uda.cl

Oswaldo Pavez

Profesor
Universidad de Atacama
Departamento de Ingeniería en Metalurgia - CRIDESAT
Copiapó - Atacama - Chile
oswaldo.pavez@uda.cl

Julia Li Kao

Profesor
Universidad de Atacama
Departamento de Química y Biología
Copiapó - Atacama - Chile
julia.li_kao@uda.cl

Amin Nazer

Profesor
Universidad de Atacama
Facultad Tecnológica
Copiapó - Atacama - Chile
amin.nazer@uda.cl

Abstract

In order to determine the exploitation potentiality of a kaolin deposit from Atacama in the north of Chile, two types of kaolin (K-1 and K-2) were characterized by XRD, XRF, SEM/EDXS, size distribution, whiteness and DSC. Kaolinite, quartz, muscovite and albite were recognized as main constituents of the ore deposit, and also a significant amount of impurities that negatively impacts on quality were detected. Results show that the low quality presented by the samples, especially K-2, impedes their industrial use as raw material and further mineral concentration processes are proposed. Finally, the results of thermal analysis confirm a conversion to metakaolin that could be the basis for an alternative processing route.

Keywords: Kaolin, X-ray diffraction, Scanning Electron Microscopy, metakaolin, DSC.

1. Introduction

Clays are one of the main components of soils and Earth crust. They have become one of the most important mineral resource of the human history, and their use goes back to ancient times (Cardarelli, 2008). One of the most important clays is kaolin, a fine grained rock that contains kaolinite ($\text{Al}_2\text{Si}_2\text{O}_5(\text{OH})_4$) as the main constituent. It has low contents of iron and other im-

purities that can turn color from white to brown, grey, or red, depending on the impurities existing in it. Kaolinite is the most common of kaolin group minerals (kaolinite, dickite, nacrite and halloysite), all these compounds excluding hydrated halloysite ($\text{Al}_2\text{Si}_2\text{O}_5(\text{OH})_4 \cdot 2\text{H}_2\text{O}$) have identical chemical composition, differing only in their structure (Guggenheim *et al.*, 1997,

Bentabol 2003). The crystal structure of the kaolin group is formed by SiO_2 tetrahedron and Al_2O_3 octahedron layers connected by oxygen and hydroxyl groups (1:1 layered clay), as shown in Figure 1. The theoretical composition of kaolinite is 46.54% SiO_2 ; 39.50% Al_2O_3 and 12.96% H_2O , and it has an earthy fracture and pseudo-hexagonal flaky morphology (Murray, 2007).

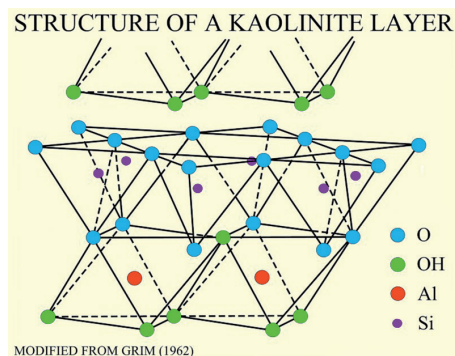


Figure 1
Kaolinite crystal structure (Credit: U.S. Geological Survey).

Due to its physical and chemical properties, kaolin can be used in a wide range of applications, such as: ceramics manufacturing, refractory products, paper industry and rubbers and plastics, among others (Luz *et al.*, 2005). Kaolin is also processed by roasting to obtain metakaolin, an amorphous aluminosilicate widely used in the construction industry (Murray, 2007)

Kaolin production in Chile is led by the Coquimbo, Metropolitana

and Libertador General Bernardo O'Higgins regions. In 2012, national production was 60,249 tons; this value has not increased from 2010 until today (Servicio Nacional de Geología y Minería – SERNAGEOMIN, 2013). In Atacama, kaolin production gradually decreased from 1999 to 2003 and there are no records of production in the last 12 years. However, there are unexploited deposits which could be potentially exploited. In addition to the above, there are no records in lit-

erature about kaolin from Atacama, neither about chemical or physical properties nor about impurities that could affect its quality or commercial value. In other words, there is no information about the kaolin of this zone.

In view of the foregoing, this study is expected to provide useful information to develop an alternative metallurgical processing, in order to make kaolin from Atacama more competitive in the local market.

2. Materials and methods

2.1 Materials

Representative samples were extracted by sorting from a deposit located in Cuesta Pajonales, in the south of Atacama. Two types of samples

were obtained and labeled K-1 (white sample) and K-2 (light brown sample) due to their predominant color. Both samples were processed by jaw and

roll crushing (100% under 100# Tyler) and the ultrafine fraction (90% under 325# Tyler) was removed by wet sieving.

2.2 Methods

X-Ray Diffraction (XRD) was carried out in a Shimadzu XRD-6100 (Cu K α) diffractometer. Step size of 0.02°, scan speed of 2 degree min⁻¹ and 2 θ from 5 to 90°.

Chemical composition was determined by X-ray fluorescence (XRF), loss of calcining at 980 °C for 1 hour and humidity at 105 °C for 1 hour.

Particle size distribution was measured in a Malvern Mastersizer analyzer. A Whiteness test was carried out by a Minolta CR-14 colorimeter with ASTM E-313 and HUNTER whiteness standards.

Morphological and chemical characterizations were carried out by Scanning Electron Microscopy (SEM) and Energy Dispersive X-Ray Spectroscopy (EDXS) in

a Zeiss EVO MA 10 with Oxford X-Max 20 detector. Secondary (SE) and backscattered (BSE) electrons modes were used for the analyses.

A TA Instruments Q20 (N₂ atmosphere) was used for Differential Scanning Calorimetry (DSC) analysis. Both samples were heated twice from 50 to 600 °C with a heating rate of 10 °C min⁻¹.

3. Results

3.1 Sample Characterization

X-ray Diffraction

XRD patterns of K-1 and K-2 are shown in Figure 2, which have been normalized for easier phase identification. Both samples present

the same mineralogical composition, being the main components kaolinite, quartz, albite and muscovite. In K-1, higher peaks of kaolinite and lower

peaks of albite are noted; this could be an indication of a higher proportion kaolinite/albite in K-1, in comparison to K-2.

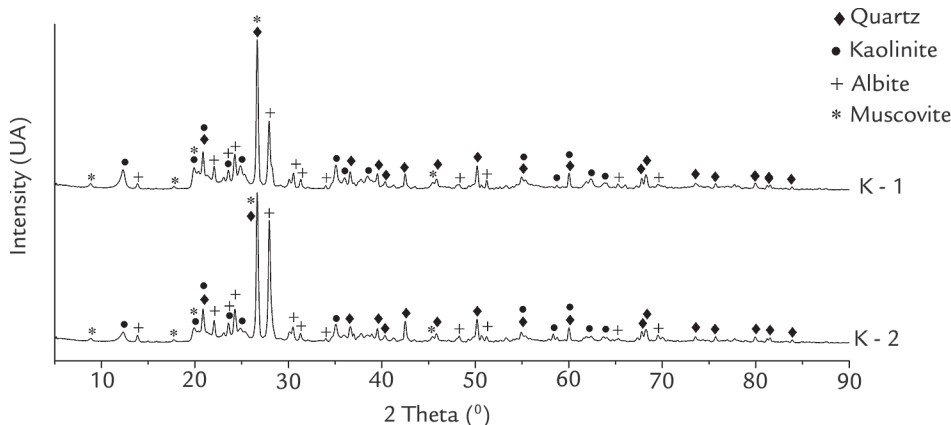


Figure 2
XRD patterns of K-1 and K-2.

X-ray Fluorescence

Table 1 shows chemical composition of K-1 and K-2, appreciable amounts of impurities in both sam-

ples are detected. Also, it should be noted that a fraction of measured SiO₂ belongs to the silicon oxide detected

by XRD.

When compared with commercial kaolinite ores, K-1 and especially

K-2 present high amounts of common impurities associated to their natural condition, and therefore a very low

quality. The impurities are detrimental for commercialization, due to the need of improving the product by

beneficiation processes to become suitable for industrial use (Yoon and Shi, 1986).

Sample	SiO ₂ (%)	Al ₂ O ₃ (%)	Fe ₂ O _{3-T} (%)	CaO (%)	MgO (%)	K ₂ O (%)
K-1	49.47	30.85	4.10	0.50	0.60	1.24
K-2	52.87	27.62	4.59	0.46	0.51	1.55

Table 1
Chemical composition of samples by XRF.

Whiteness test

Whiteness results are presented in Table 2. Both samples present low values, in particular K-2, considering that mar-

ketable values for commercial kaolin are above 90 for ASTM E 313, and around 82.5% for HUNTER standard. As ad-

ditional data, paper industry demands an ISO whiteness index above 84.5% (Moraes et al., 2001, Costa, et al., 2009).

Sample	ASTM E 313	HUNTER
K-1	53.70	79.18
K-2	26.64	70.02

Table 2
K-1 and K-2 whiteness values.

Particle size analysis

Obtained values of d50 for K-1 and K-2 were 17 and 15 μm, respectively. Moraes et al. (2001) reported that the

paper industry demands kaolin with d50 values between 2 to 10 μm, and for coating purposes under 2 μm. Results show that

K-1 and K-2 are not suitable as paint filler or coating in the paper industry, if only jaw and roll crushing stages are considered.

Scanning Electron Microscopy / Energy Dispersive X-ray Spectroscopy

Figure 3 a) and b) are SEM images (200X) in SE mode of K-1 and K-2. Both samples present a morphology

which consists of big agglomerated particles between 10 to 80 micrometers, which are formed by smaller particles

around few microns of size. Bentabol (2003) reported the same morphology for natural kaolinite.

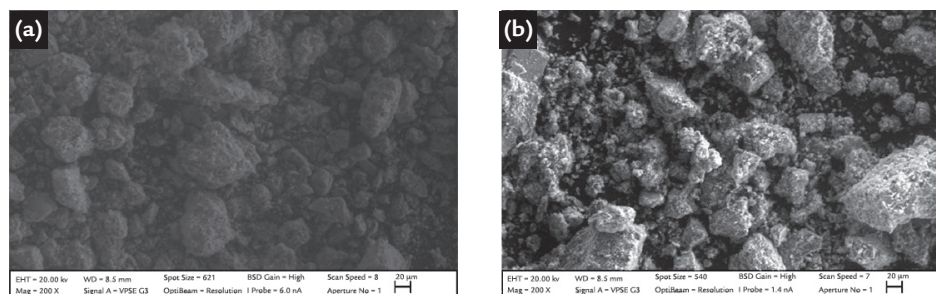


Figure 3
SEM images (200X) of a) K-1 and b) K-2.

Results of EDXS analysis are presented above; K-1 was chosen because of its higher quality, in comparison to K-2. Figure 4 presents the SE reference image (500X) of the studied zone, whereas Figure 5 presents the

elemental distribution of silicon, aluminum, titanium, potassium, oxygen, iron and sodium (as identified on the upper side of each picture). A homogeneous distribution of aluminum, silicon and oxygen is observed, and

several impurities identified as iron and titanium-rich particles are reported. On the other hand, presence of sodium and potassium is consistent with detection of albite (NaAlSi₃O₈) and muscovite (KAl₂(AlSi₃O₁₀)(OH)₂) by XRD.

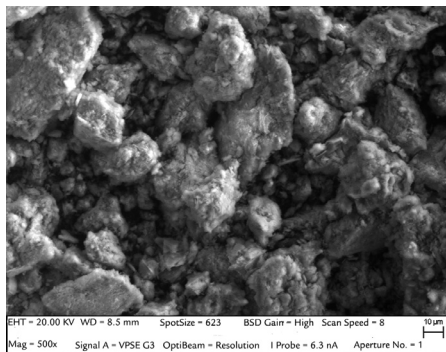


Figure 4
SE image of EDXS mapped zone (500X).

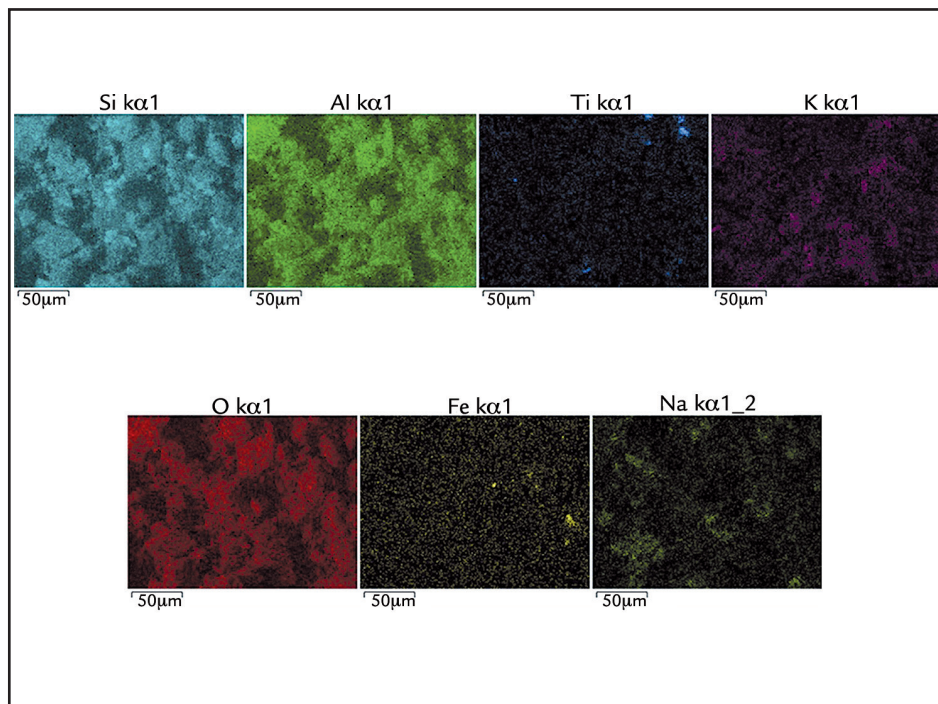


Figure 5
EDXS mapping of Figure 4.

Figure 6 shows an enlarged view (1000X) of an iron-rich particle found in K-2. A botryoidal texture, commonly presented by iron oxides like hematite or goe-

thite is observed. These oxides are found in several ore deposits in the northern side of Chile and they might be removed by metallurgical processes like dispersion,

high intensity magnetic separation, leaching or magnetic filtration, among others, to avoid detrimental effects in the kaolin quality (Luz *et al.*, 1995; Luz *et al.*, 2005).

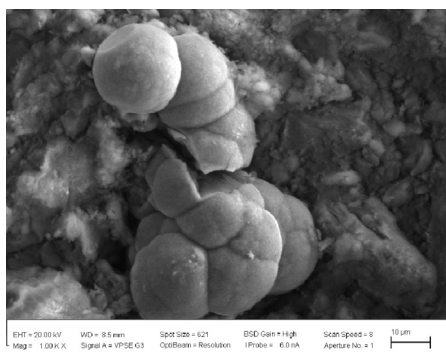


Figure 6
Iron-rich particle found in K-2 (500X).

3.2 Thermal Analysis

Differential Scanning Calorimetry

DSC results are presented in Figure 7. Both samples show one irreversible endothermic reaction around 500 °C, which is consistent with the kaolin dehydroxylation temperature (Redfern, 1987). DSC curves and calculated en-

thalpies (220.2 Jg⁻¹ for K-1 and 126.7 Jg⁻¹ for K-2) show that K-1 requires more energy to achieve the endothermic reaction. If we consider the above and take into account that specialized bibliography confirms that kaolinite DSC

curves mainly depend on a) particle size, b) impurities, c) heating rate and d) degree of crystallinity/disorder, it could be supposed that there is a higher degree of crystallinity or kaolinite content for K-1, in comparison to K-2 (Redfern, 1987).

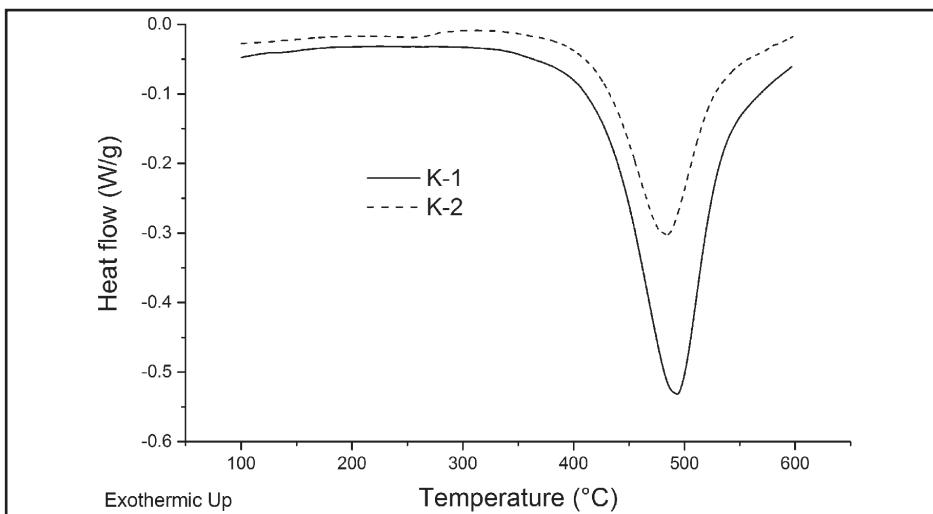


Figure 7
DSC curves of K-1 and K-2.

In order to analyze the effects of heating on the studied samples, XRD patterns before and after DSC are presented in Figures 8 and 9. After DSC, the main peaks of kaolinite in both

samples disappear and the remaining kaolinite peak heights decrease. This can be explained by kaolinite conversion to metakaolin, which is accomplished by an amorphization process.

After heating, K-1 presents a hump in range $2\theta = 20$ to 30° , this is an evidence of system amorphization and also suggests a higher content of crystalline kaolinite in K-1.

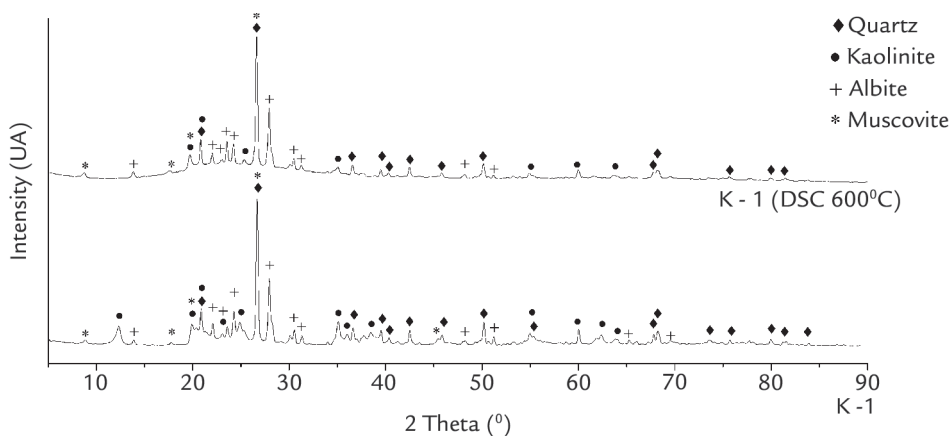


Figure 8
K-1 raw and heated XRD patterns.

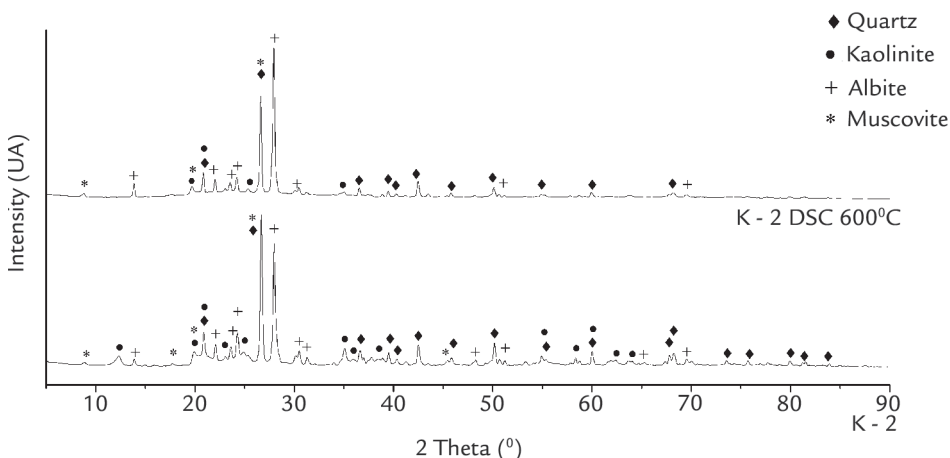


Figure 9
K-2 raw and heated XRD patterns.

4. Conclusions

The studied samples cannot be commercialized directly without further comminution and metallurgical processing stages. Considering the impurities of both samples, a wet treatment consisting of dispersion, high intensity magnetic separation, leaching or magnetic filtration is proposed.

Metallurgical parameters such as mineral composition, whiteness, kaolinite content and degree of kaolinite crystallinity, suggest that K-1 presents the highest exploitation potential of the studied samples.

Despite the samples having been heated up to 600°C and immediately

cooled down to room temperature, it was observed that the main peaks of kaolinite disappeared. It is suggested that a thorough study must be made, in order to lead to new alternative processing routes for the studied ore deposit.

5. Acknowledgements

The authors thank the support of Research and Postgraduate Directorate of Universidad de Atacama for funding DIUDA 221213 project. The authors

also gratefully appreciate the research assistance from Laboratorio de Materiales and the collaboration of Miss Evelyn Cárdenas for the reviewing of

this article, both from Departamento de Ingeniería en Metalurgia, Universidad de Atacama.

6. References

- BENTABOL, M. J. *Transformaciones hidrotermales de la caolinita*. Facultad de Ciencias, Universidad de Málaga, 2003. 395 f. (Tese de Doutorado).
- CARDARELLI, F. *Materials handbook. A concise desktop reference*. (2. Ed.). Springer-Verlag London Limited, 2008. 1340p.
- COSTA, D. S., RUSSO, M. C., SANTOS, D.F., ARAUJO, A.C., PERES, A.E.C. (2009). Avaliação do potencial de superfície de partículas de caulim proveniente da região nordeste de Minas Gerais. In: ENCONTRO NACIONAL DE TRATAMENTO DE MINÉRIOS E METALURGIA EXTRATIVA, 23. *Anais...* Gramado, 27 set. - 1º out. 2009. v2, p.569-574.
- GUGGENHEIM S., ALIETTI A., DRITS V. A., FORMOSO M. L. L., GALÁN E., KÖSTER H. M., PAQUET H., WATANABE T., BAIN D. C., HUDNALL W. H.. Report of the Association Internationale Pour L'Etude des Argiles (AIPEA) Nomenclature Committee for 1996. *Clays and Clay Minerals*, v. 45, n. 2, p. 298-300, 1997.
- LUZ A. B., CAMPOS A. R., CARVALHO E. A., BERTOLINO L. C. Caulim. In: LUZ A. B., FREITAS LINS F. (ed.) *Rochas e Minerais Industriais*. Rio de Janeiro: CETEM/MCT, 2005. p. 231-262. 720. (Cap. 11).
- LUZ, A.B., COSTA, L.N.S., CHAVES, A.P. Aspectos de alguns redutores usados no alvejamento de caulins. In: XVI ENCONTRO NACIONAL DE TRATAMENTO DE MINÉRIOS E METALURGIA EXTRATIVA, 16. Rio de Janeiro, 1995, v. 1, p.163-179.
- MORAES J. M., LUZ A. B., BERTOLINO, L.C. Caracterização tecnológica e mineralógica de caulins brasileiros. In: JORNADA DE INICIAÇÃO CIENTÍFICA, 14. Rio de Janeiro: CETEM/MCT, 2006.
- MURRAY H. H. *Applied clay mineralogy*. Occurrences, processing and application of kaolins, bentonites, palygorskite-sepiolite and common clays. Elsevier, 2007. 180p.
- REDFERN S. A. T. The kinetics of dehydroxylation of kaolinite. *Clay Minerals*. v. 22, n. 4, p. 447-456, 1987.
- YOON R., SHI J. Processing of kaolin clay. In: SOMASUNDARAN, P. (Ed.). *Advances in Mineral Processing*. New York: American Institute of Mining, Metallurgical and Petroleum Engineers, AIME, 1986.

Received: 14 January 2016 - Accepted: 11 July 2016.